Scientific Research Publishing

New Journal of Glass and Ceramics, 2026, 14(1), 1-14
https://www.scirp.org/journal/njgc
ISSN Online: 2161-7562
ISSN Print: 2161-7554

Incorporation of Spent Pot Lining in Ceramic Masses

Venildo Mussane[1], Aluai Buraimo[1], Carvalho Madivate[2], Arão Manhique[1], Fabio Attore[3], Alcides Sitoe[1]*

[1]Department of Chemistry, Eduardo Mondlane University, Maputo, Mozambique
[2]Instituto Superior de Ciências e Tecnologia (ISCTEM), Maputo, Moçambique
[3]Department of Environmental Biology, Sapienza Universita de Roma, Rome, Italy
Email: *alcides.sitoe@gmail.com

How to cite this paper: Mussane, V., Buraimo, A., Madivate, C., Manhique, A., Attore, F. and Sitoe, A. (2026) Incorporation of Spent Pot Lining in Ceramic Masses. *New Journal of Glass and Ceramics*, **14**, 1-14.
https://doi.org/10.4236/njgc.2026.141001

Received: May 18, 2026
Accepted: July 25, 2026
Published: July 28, 2026

Abstract

The aluminium industry has expressed, in recent years, a high growth rate. During aluminium production, several solid wastes are generated. The ceramic industry has great potential for the reuse of waste because it can incorporate heterogeneous waste from different origins and compositions without a significant depreciation of its product quality. Mozambique Aluminium (MOZAL) generates 5 tons/day of residue and a viable method for its disposal has not yet been found. The main objective of the present work is to develop an alternative for the reuse of the spent pot lining (SPL) residue from the production of carbon anodes at the MOZAL factory. The use of the waste was promoted through its incorporation into ceramic masses. For this purpose, the effect on linear shrinkage, weight loss, bulk density, water absorption and compressive strength was evaluated by varying the firing temperature (850 to 950˚C), firing time (15 to 45 minutes) and SPL content (0 to 20%). The minimum values established by the NM 127 2009 standard were compared with the results obtained from the compressive strength in the partial replacement of clay by SPL. The optimal processing conditions were found to be firing at 900˚C for 30 minutes with 10% of SPL content. The incorporation of SPL up to 15% has a positive influence and can be used to produce solid bricks (up to 10% for all classes and 15% for B and C classes). However, it is recommended that replacements do not exceed 15% to ensure good resistance results according to the minimum values.

Keywords

Clay, Ceramic Mass, SPL Residue, Carbon Anodes

1. Introduction

Worldwide in 2019 about 64 million metric tons of aluminium were produced. Globally, about 1.7 million tons of spent pot lining (SPL) are generated annually. The generation of SPL is around 25 kg per ton of primary aluminium production. The SPL produced is divided into two fractions: carbonaceous part and non-carbonaceous part (refractory based). The carbonaceous part accounts for about 55% of the total weight of the SPL materials [1]-[4].

Spent pot lining is a toxic waste material resulting from aluminium smelters after 3 - 8 years of operation. It contains water-soluble fluorides and cyanides, which contribute to soil and water pollution [5]-[9].

Due to the negative environmental impact of its disposal without a beneficiation process, efforts are being made to study forms of its treatment before disposal. Results presented in the literature show different forms of its treatment. One of the examples is the chemical processing of the residue by transforming it into a non-toxic substance or its inertization that can be used as alternative energy source. Based on the high content of carbonaceous material the residue can be used as supplementary raw material in cement and ceramic industry as well as recovery of valuable components present in the residue. Some of the processes used for the treatment of SPL waste make use of a plant for processing the waste [2] [10]-[16].

In research motivated by high prices and problems associated with the supply of coal raw materials, [17] studied the potential use of SPL as an alternative material in iron production. Its use brought benefits in terms of energy consumption and emission of sulphur compounds but presupposes a beneficiation process before its use because of the high contents of cyanide and ashes. Reference [11] reports recovery of some valuable components through a multistep washing process, involving a water wash followed by acid wash. Since this process involves the use of a plant, larger companies may practice it with large amounts of SPL generated.

The use of SPL is beneficial in the ceramic industry where the inorganic fraction of produced slags reacts with ceramic masses. Furthermore, combustion of the carbon fraction of the SPL contributes to better burning of the ceramic material and increases the porosity [5].

Part of the fluorides present in SPL can be stabilized by reaction with CaO and SiO_2 present in ceramic masses through formation of $3CaO{\cdot}2SiO_2{\cdot}CaF_2$ [13] [18] [19], while cyanides are decomposed, delivering N_2 and CO_2, at high temperatures where burning of ceramics occurs [20]. Although leachability of fluoride in SPL samples treated at 1200˚C showed results suggesting a need for its stabilization (≈42.5 mg/l), emissions of cyanide and fluoride reported on incorporation of SPL in ceramic masses are, apparently, below limit values imposed by regulations [12], suggesting efficiency of the transformation described above on the inertization of noxious fluorides.

In the present research, the effect of SPL residue from the production of carbon anodes of Mozambique Aluminium (MOZAL) on mechanical and physical prop-

erties of OUA clay was studied. Optimization of the impact of addition of SPL was also determined, based on the compressive strength and other properties of prepared specimens.

2. Materials and Methods

2.1. Samples

Samples of clay collected in Boane district—Maputo Province (OUA clay) and SPL from MOZAL were dried and pulverized, then stored in sealed plastic bags at room temperature.

2.2. Characterization of the Samples

Chemical composition of the SPL and clay samples was determined semi-quantitatively by X-ray Fluorescence (XRF) and the mineralogical analysis was done using X-ray Diffraction (XRD) to identify the phases present in SPL samples. The Rietveld method was used to estimate the present phases. The thermal behaviour was determined using thermogravimetric analysis (TGA).

2.3. Preparation of Specimens

The clay specimens were prepared using a prismatic mould (15 × 3 × 2.5 cm). The specimens were prepared by adding SPL in contents varying between 0 and 20% (Table 1). The specimens were first dried in air at room temperature for eight days, changing the exposed side each day. The specimens were transferred to an oven, where they were dried at 105˚C for 24 hours. Firing test pieces were carried out in an electric kiln at a rate of 5˚C/min to reach the maximum temperatures of 850˚C, 900˚C and 950˚C, for a period of 15, 30 and 45 minutes and cooled to a room temperature. Five specimens were tested for each condition and the average was recorded. The electric kiln was previously calibrated, and all specimens were prepared by the same operator.

Table 1. Nominal SPL content (in wt-%) of prepared samples.

Sample	OUA Clay (%)	SPL (%)
M0	100	0
M5	95	5
M10	90	10
M15	85	15
M20	80	20

2.4. Characterization of Fired Specimens and Optimization of the Process (Firing Temperature, Composition, Firing Time)

Optimization of the process was based on results of the effect of firing temperature (850˚C to 950˚C), firing time (15 to 45 minutes) and SPL content (0 to 20%) on mechanical properties of fired masses, particularly linear shrinkage, weight loss,

compressive strength, bulk density, and water absorption.

Determination of Linear Shrinkage (LS)

To determine the linear shrinkage of dried and fired samples, the methodology by [21] was used. The length of the specimens was measured right after moulding (C_0), after drying in an oven (C_s) and after firing (C_q) in an electric kiln. Equations (1) and (2) were used to calculate the Linear Drying Shrinkage (LDS) and the Linear Firing Shrinkage (LFS), respectively. Length measurements were performed using a digital Vernier calliper (resolution ± 0.001 mm).

$$\mathrm{LDS}(\%) = \frac{C_0 - C_s}{C_0} \times 100 \tag{1}$$

$$\mathrm{LFS}(\%) = \frac{C_s - C_q}{C_s} \times 100 \tag{2}$$

Determination of Weight Loss (WL)

To determine the WL, the methodology used by [22] was followed. The specimen was weighed after drying in an oven (m_2) and after firing (m_3). Equation (3) was used to determine Weight Loss (WL).

$$\mathrm{WL}(\%) = \frac{m_2 - m_3}{m_2} \times 100 \tag{3}$$

Determination of Bulk Density (BD)

To determine the BD, the methodology by [23] was used. The specimen was weighed after firing (m_3, in g) and the specimen volume was determined from the dimensions of the specimen after firing (V, in cm^3) with the aid of a digital Vernier calliper (resolution ± 0.001 mm). Equation (4) was used to calculate the bulk density (AD).

$$\mathrm{DA}\left(\frac{\mathrm{g}}{\mathrm{cm}^3}\right) = \frac{m_3}{V} \tag{4}$$

Determination of Water Absorption (WA)

To determine the WA, the methodology used by [24] was followed. The fired specimen was weighed after drying in an oven at 105˚C for 24 hours (m_3) and it was weighed after resting the specimen in water for 24 hours (m_4) after removing excess surface water with a cloth.

$$\mathrm{WA}(\%) = \frac{m_4 - m_3}{m_4} \times 100 \tag{5}$$

Determination of Compressive Strength (CS)

To determine the CS, the methodology used by [22] was followed. First, with the aid of a digital vernier caliper the edge of the specimen (a) was measured in cm and the area of the specimen section (A) in cm^2 was calculated and the compressive strength tests were performed in a Press (brand: AMSLER, model: SCHAFF-HOUSE-SUISSE 699/365) with loading rate of 0,6 MPa/s. Equation (6) was applied to determine the CS.

$$\mathrm{CS}(\mathrm{MPa}) = \frac{F(\mathrm{kg_f})}{A(\mathrm{cm^2})} \times 0.0981 \quad (6)$$

3. Results and Discussion

3.1. Characterization of the Samples

Table 2 presents results of the chemical composition of OUA clay and SPL, while Table 3 and Table 4 present mineralogical compositions of OUA clay and SPL. Chemical analyses were performed by XRF, which is insensitive to light elements such as carbon and fluorine; therefore, the results of the chemical composition of SPL in Table 2 do not include coal content.

Clay is composed essentially of silica and alumina or magnesia and water, but iron replaces aluminium and/or magnesium in several positions, and appreciable amounts of potassium, sodium and calcium are often present. Expectedly, these results revealed high Si, Al and Fe contents, consistent with the fact that clay minerals are phyllosilicates. This clay sample presented the higher content of iron. This element provides reddish tones after firing the ceramic mass [25] [26].

Table 2. Chemical composition (%) of OUA clay and spent pot lining.

Components	OUA Clay	SPL
Si	48.851	2.191
K	4.324	0.272
Fe	23.882	31.319
Ca	2.438	6.559
Ti	2.191	---
Al	16.695	38.231
Mn	0.554	0.360
S	0.428	18.61
Zr	0.169	---
V	0.123	0.190
Cr	0.086	0.045
Cu	0.079	0.142
Sr	0.077	0.233
Zn	0.041	0.037
Y	0.029	---
As	---	0.112
Ir	---	0.035
Ni	---	1.656
Pb	---	0.010
Se	---	0.003

The results of XRD revealed that OUA clay is predominantly composed of quartz, plagioclase, corundum, and muscovite as main phases (Table 3). These phases are related to the high amounts of the elements silicon, aluminium and iron.

Table 3. Mineralogical composition of OUA Clay.

Components		Content (%)
Quartz	(SiO_2)	40.00
Corundum	(Al_2O_3)	12.60
Plagioclase	($NaAlSi_3O_8$-$CaAl_2Si_2O_8$)	27.00
Microcline	($KAlSi_3O_8$)	11.60
Muscovite	[$KAl_2(AlSi_3O_{10})(F,OH)_2$]	6.50
Cordierite	[$(Mg,Fe)_2Al_4Si_5O_{18}$]	0.70
Hematite	(Fe_2O_3)	1.70

The XRD results showed that the SPL sample has expectedly high contents of graphite, cryolite and alumina (Table 4). Apart from the carbon and fluorine content the chemical composition of SPL showed presence of aluminium. Iron and sulphur, with relatively small amounts of calcium, silicon and nickel were also present [4] [16].

Table 4. Mineralogical composition of Spent pot lining.

Components		Content (%)
Graphite	(C)	77.06
Cryolite	[$Na_3(AlF_6)$]	10.82
Chiolite	($Na_5Al_3F_{14}$)	6.74
Alumina	(Al_2O_3)	5.07
Magnesium ferrite	($MgFe_2O_4$)	0.32

Figure 1 and Figure 2 show the thermal behaviour of OUA clay and SPL, respectively. TGA was used to characterize the thermal behaviour of the clay samples. The TGA was carried out with a TA Instrument SDT-Q600 Simultaneous/DSC. Samples weighing approximately 15 - 20 mg were heated from ambient temperature to 900˚C at a heating rate of 10 K/min under an inert atmosphere (nitrogen) and air at a flowing rate of 100 mL/min. Diagram in Figure 1 show the typical water loss of a clay (starting at temperature below 100˚C) with a further weight loss extending up to 600˚C, which includes the firing of organic matter. Figure 2 shows a large weight loss peak in the interval 500˚C - 800˚C associated with carbon combustion in air atmosphere (Sun *et al.*, 2019; Sun *et al.*, 2021). Carbon combustion easily occurred in the oxidative atmosphere. Similar results were also reported by [20], comparing 70% CO_2/30% O_2 and 70% N_2/30% O_2 atmos-

pheres. In the inert atmosphere, the mass loss was less than 5%, which may result from the decomposition of cryolite [20].

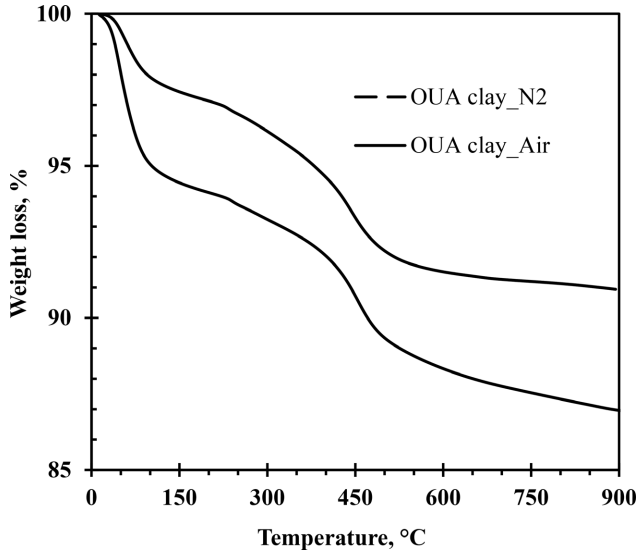

Figure 1. Thermogravimetric analysis of the OUA clay.

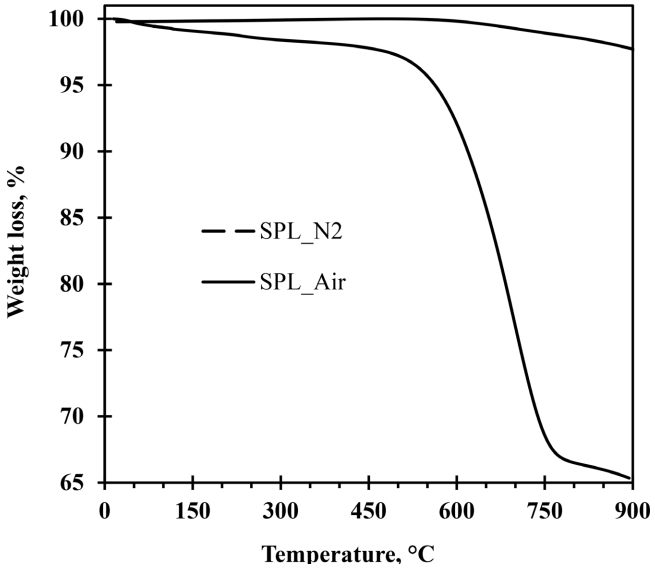

Figure 2. Thermogravimetric analysis of the spent pot lining.

3.2. Characterization of Fired Specimens and Optimization of the Process

Firing temperature

Figure 3 presents results of the effect of firing temperature on properties of fired masses with 10% SPL fired for 30 minutes. Increasing the firing temperature, the linear shrinkage increases up to 900˚C; after this temperature, it drops. It would be expected that with increasing temperature the shrinkage would increase because of the removal of volatile or organic matter. But it is important to consider that the increase in temperature can favour the dilation of the pores, improving the

exposure of the organic material to air, thus allowing it to burn. This burning will produce gases that will increase porosity, which increases the volume of the specimens.

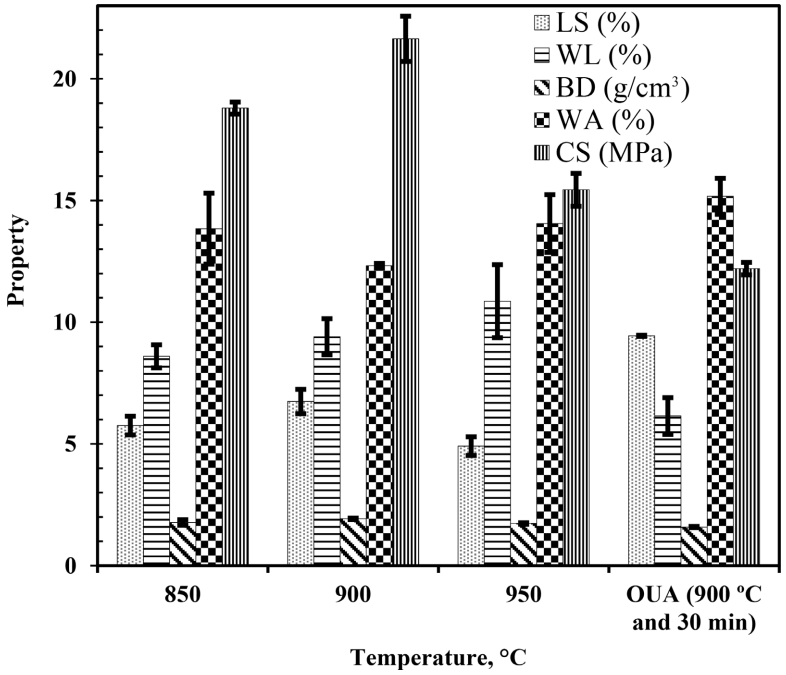

Figure 3. Effect of firing temperature on properties of OUA clay with 10% spent pot lining fired for 30 minutes. (LS: Linear Shrinkage, WL: Weight Loss, BD: Bulk Density, WA: Water Absorption and CS: Compressive Strength).

This observation is confirmed by the appearance of the specimens shown in Figure 4; specimens fired at 950˚C have a high porosity and greater volume compared to those produced at lower temperatures. This behaviour was also observed by [22]. Weight loss increases with the increase in firing temperature. Reference [27] found similar results. According to the authors, weight loss increases due to the increase in water loss associated with hydroxides, clay mineral water, loss of volatile material and burning of organic material during the firing process.

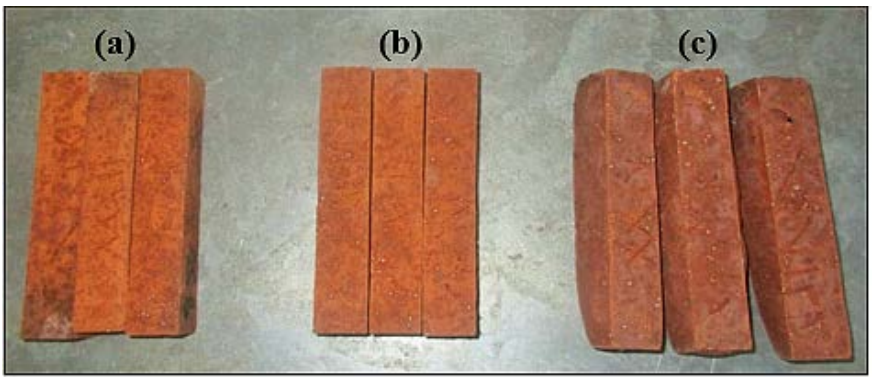

Figure 4. Visual appearance of specimens fired at (a) 850, (b) 900 and (c) 950˚C for 30 minutes with 10% spent pot lining.

From the results in Figure 3, a firing temperature of 900˚C was selected as the optimal one and was used in further experiments. Samples fired at 900˚C show the highest compressive strength values and the lowest water absorption. Firing of specimens at temperatures higher than 900˚C introduces deformation of fired material (Figure 4), which may have contributed to the reduction of compressive strength and the increase of water absorption values and linear shrinkage.

Firing time

Effect of time of firing on specimens with 10% SPL, carried out at 900˚C, is presented in Figure 5. Linear shrinkage increased with increasing burning time; a fact also observed by [27].

Although firing time of 45 minutes gave best values of the compressive strength, optimal time selected was 30 minutes, since specimens fired at 45 minutes causes cracks and warping (Figure 6). Increased weight loss and improved water absorption and compressive strength are a result of a better completion of the transformations taking part during firing of the material, including a higher degree of

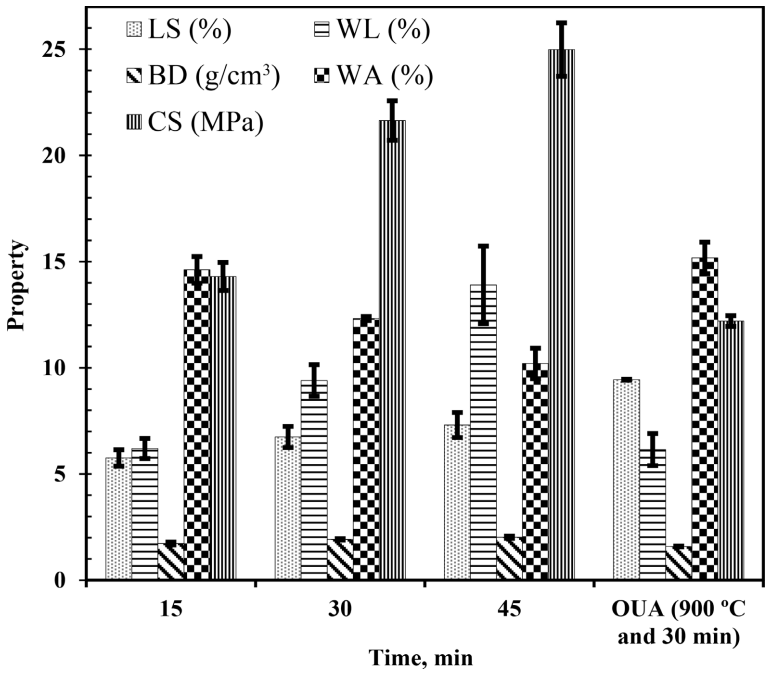

Figure 5. Effect of firing time on properties of clay with 10% spent pot lining, fired at 900˚C. (LS: Linear Shrinkage, WL: Weight Loss, BD: Bulk Density, WA: Water Absorption and CS: Compressive Strength).

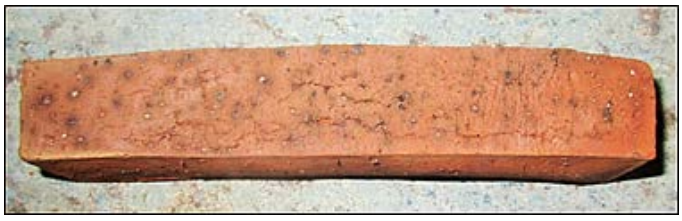

Figure 6. Visual appearance of specimens fired at 900˚C for 45 minutes with 10% spent pot lining.

vitrification of fired clay [27].

SPL content

Figure 7 presents properties of fired clay masses with different amounts of spent pot lining in the range of 0 to 20%, fired for 30 minutes at 900˚C. This temperature and time were observed to be those that produce specimens with the best properties. The replacement of clay by SPL caused a reduction in shrinkage; this behaviour was also observed by [28] in the incorporation of waste clay ceramics from a water treatment plant. The continuous addition of SPL resulted in an increase in weight loss. Increased weight loss is explained hereby, particularly by the combustion of organic matter present in the SPL [22] [27]. With increasing percentage of SPL, the bulk density and water absorption decreased to 10%, then increased. This property confirms the behaviour of bulk density because, according to [29], the higher the density, the lower the water absorption.

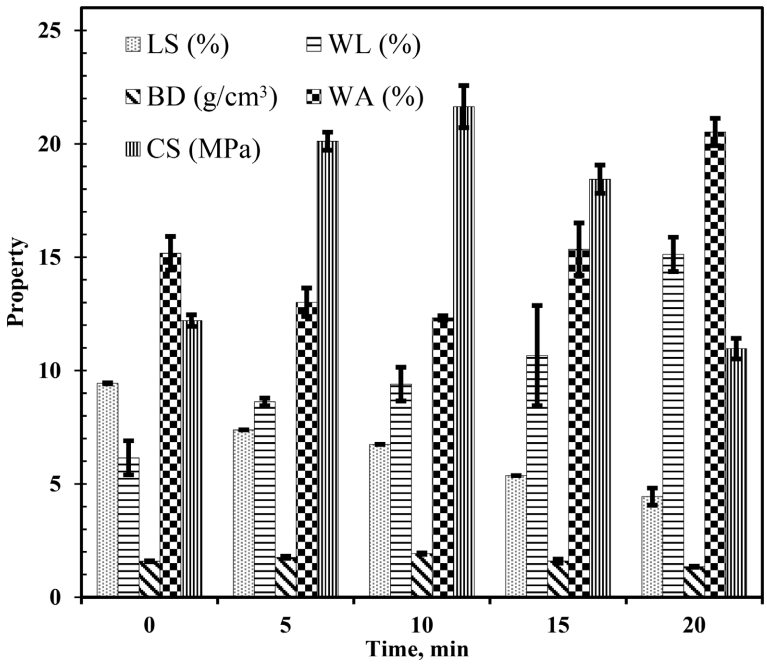

Figure 7. Properties of fired clay masses with increasing amounts of spent pot lining, fired for 30 minutes at 900˚C. (LS: Linear Shrinkage, WL: Weight Loss, BD: Bulk Density, WA: Water Absorption and CS: Compressive Strength).

Water absorption and compressive strength registered an optimal value at 10% spent pot lining addition. Figure 8 shows the comparison between the minimum values established by the [30] standard to produce solid bricks and the compressive strength values in the partial replacement of clay by the SPL residue. Clay masses with 5% and 10% SPL can be used in the production of solid bricks of all classes (A, B and C), while clay masses with 15% can be used for the production of solid bricks of category B and C. Clay masses with 20% cannot be used for the production of solid bricks as it does not have strength within the acceptable limit.

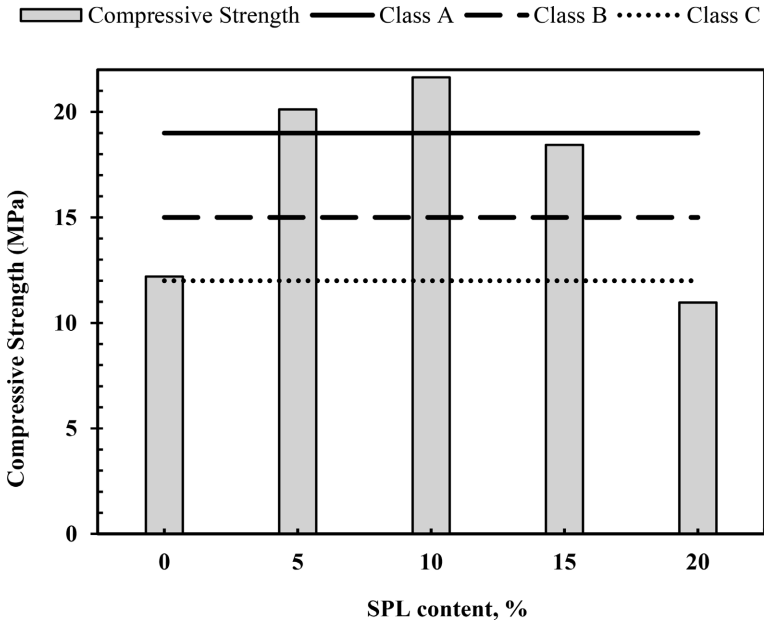

Figure 8. Comparison of compressive strength values with values for solid bricks (norm NM 127 2009).

4. Conclusion

In the present work, a viable alternative was developed for the use of residue (SPL) from Mozambique Aluminium (MOZAL), which in the future could bring environmentally sustainable benefits and lower operating costs. For this objective, the effect on linear shrinkage, weight loss, bulk density, water absorption and compressive strength was evaluated by varying the firing temperature (850˚C to 950˚C), firing time (15 to 45 minutes) and SPL content (0 to 20%). The firing temperature of 900˚C and the firing time of 30 minutes with 10% residue promoted the best results; as a result, they were found to be the optimal conditions, with values of linear shrinkage, weight loss, bulk density, water absorption and compressive strength equal to 6.74%, 9.40%, 1.93 g/cm^3, 12.32% and 21.64 MPa, respectively. The incorporation of residue from the production of carbon anodes has a positive influence up to 15% addition on the physical and mechanical properties of ceramic masses. These clay masses can be used to produce solid bricks of categories A, B and C. However, it is recommended that replacements do not exceed 15% to ensure good resistance results according to the minimum values established by the [30] standard.

Conflicts of Interest

The authors declare no conflicts of interest regarding the publication of this paper.

References

[1] Agrawal, A., Kumar, C. and Meshram, A. (2021) Recovery of Carbon Rich Material: -Recycling of Spent Pot Lining: A Review. *Materials Today*: *Proceedings*, **46**, 1526-1531. https://doi.org/10.1016/j.matpr.2021.01.143

[2] Chen, Y., Li, P., Bu, X., Chehreh Chelgani, S., Kong, Y. and Liang, X. (2022) Resource Utilization Strategies for Spent Pot Lining: A Review of the Current State. *Separation and Purification Technology*, **300**, Article 121816. https://doi.org/10.1016/j.seppur.2022.121816

[3] Khan, M.S. and Chen, X. (2025) Hybrid Experimental-DFT Studies on Sustainable Production of Nepheline Ceramics from Hazardous Spent Potlining Residues. *Ceramics International*, **51**, 47895-47904. https://doi.org/10.1016/j.ceramint.2025.08.048

[4] Ansari, K., Siddique, S., Shahzad, S., Khalid, H.R. and Hanif, A. (2026) Efficient Utilisation of Spent Pot Lining, Aluminium Dross and Red Mud as Supplementary Cementing Materials: A Comprehensive Review. *European Journal of Environmental and Civil Engineering*, **30**, Article 2617992. https://doi.org/10.1080/19648189.2026.2617992

[5] Sun, G., Zhang, G., Liu, J., Evrendilek, D.E. and Buyukada, M. (2021) Thermal Behaviors, Combustion Mechanisms, Evolved Gasses, and Ash Analysis of Spent Potlining for a Hazardous Waste Management. *Journal of Environmental Sciences*, **107**, 124-137. https://doi.org/10.1016/j.jes.2021.02.003

[6] Zhao, H., Liu, F., Xie, M., Liu, W. and Sohn, H.Y. (2021) Recycling and Utilization of Spent Potlining by Different High Temperature Treatments. *Journal of Cleaner Production*, **289**, Article 125704. https://doi.org/10.1016/j.jclepro.2020.125704

[7] Brial, V., Tran, H., Sorelli, L., Conciatori, D. and Ouellet-Plamondon, C.M. (2022) Improvement of Treated Spent Pot Lining Reactivity in Cementitious Material by Calcination. *Developments in the Built Environment*, **12**, Article 100098. https://doi.org/10.1016/j.dibe.2022.100098

[8] Shirmahd, H., Jamavari, A. and Adeli, M. (2023) Recycling of Spent Pot Lining (SPL) from Aluminum Smelters by Water Leaching. *International Journal of Environmental Science and Technology*, **20**, 11427-11436. https://doi.org/10.1007/s13762-023-05163-6

[9] Sathish, T., Saravana, R., Giri, J., Ubaidullah, M., Shangdiar, S., Kadhila, T., *et al.* (2025) Sustainable Treatment of Hazardous Spent Pot Lining Waste from Aluminum Manufacturing through Optimized Alkali and Acid Leaching. *Environmental Technology & Innovation*, **37**, Article 103973. https://doi.org/10.1016/j.eti.2024.103973

[10] Ghenai, C., Inayat, A., Shanableh, A., Al-Sarairah, E. and Janajreh, I. (2019) Combustion and Emissions Analysis of Spent Pot Lining (SPL) as Alternative Fuel in Cement Industry. *Science of The Total Environment*, **684**, 519-526. https://doi.org/10.1016/j.scitotenv.2019.05.157

[11] Pong, T.K., Adrien, R.J., Besida, J., O'Donnell, T.A. and Wood, D.G. (2000) Spent Potlining—A Hazardous Waste Made Safe. *Process Safety and Environmental Protection*, **78**, 204-208. https://doi.org/10.1205/095758200530646

[12] Samec, N., Mikša, D. and Kokalj, F. (2004) Recycling Possibilities of Spent Potlining from the Aluminum Industry (Vol. 78). WIT Press.

[13] Xie, W., Zhou, F., Liu, J., Bi, X., Huang, Z., Li, Y., *et al.* (2020) Synergistic Reutilization of Red Mud and Spent Pot Lining for Recovering Valuable Components and Stabilizing Harmful Element. *Journal of Cleaner Production*, **243**, Article 118624. https://doi.org/10.1016/j.jclepro.2019.118624

[14] Brial, V., Tran, H., Sorelli, L., Conciatori, D. and Ouellet-Plamondon, C.M. (2021) Evaluation of the Reactivity of Treated Spent Pot Lining from Primary Aluminum Production as Cementitious Materials. *Resources, Conservation and Recycling*, **170**, Article 105584. https://doi.org/10.1016/j.resconrec.2021.105584

[15] Dzikunu, P., Arthur, E.K., Gikunoo, E., Bleppony, E., Agyemang, F.O. and Mensah-Darkwa, K. (2023) Successive Selective Leaching Procedures for Valorization of Spent Pot Lining Carbon. *Process Safety and Environmental Protection*, **169**, 1-12. https://doi.org/10.1016/j.psep.2022.11.008

[16] Han, F., Yu, L., Zhang, L., Jia, J. and Dong, J. (2024) Synergistic Reutilization of Spent Pot Lining and Water Quenched Blast Furnace Slag as Mold Flux. *Process Safety and Environmental Protection*, **190**, 625-634. https://doi.org/10.1016/j.psep.2024.07.071

[17] Flores, I.V., Fraiz, F., Lopes Junior, R.A. and Bagatini, M.C. (2019) Evaluation of Spent Pot Lining (SPL) as an Alternative Carbonaceous Material in Ironmaking Processes. *Journal of Materials Research and Technology*, **8**, 33-40. https://doi.org/10.1016/j.jmrt.2017.11.004

[18] Li, R., Lu, T., Xie, M. and Liu, F. (2020) Analysis on Thermal Behavior of Fluorides and Cyanides for Heat-Treating Spent Cathode Carbon Blocks from Aluminum Smelters by TG/DSC-MS & ECSA®. *Ecotoxicology and Environmental Safety*, **189**, Article 110015. https://doi.org/10.1016/j.ecoenv.2019.110015

[19] Wang, Y., Chen, X., Zhang, S. and Yang, P. (2020) Recycling of Spent Pot Lining First Cut from Aluminum Smelters by Utilizing the Two-Step Decomposition Characteristics of Dolomite. *Materials*, **13**, Article 5283. https://doi.org/10.3390/ma13225283

[20] Sun, G., Zhang, G., Liu, J., Xie, W., Kuo, J., Lu, X., *et al.* (2019) Thermogravimetric and Mass-Spectrometric Analyses of Combustion of Spent Potlining under N_2/O_2 and CO_2/O_2 Atmospheres. *Waste Management*, **87**, 237-249. https://doi.org/10.1016/j.wasman.2019.01.047

[21] Fabris, D.C.N., Silva, J.R.d., Rodrigues, A.P., Montedo, O.R.K. and Noni, A.D. (2017) Efeito de aditivo defloculante no processamento de massa para a obtenção de blocos cerâmicos estruturais. *Cerâmica Industrial*, **22**, 31-36. https://doi.org/10.4322/cerind.2017.004

[22] Gaspareto, M.G.T. and Teixeira, S.R. (2017) Utilização de residuo de construção civil e demolição (RCD) Como material não plástico para a produção de tijolos cerâmicos. *Cerâmica Industrial*, **22**, 40-46. https://doi.org/10.4322/cerind.2017.014

[23] Cerqueira, N.A., Alexandre, J., Xavier, G.C., Souza, V.B. and Azevedo, A.R.G. (2017) Comportamento físico e mecânico de blocos prensados e queimados de cerâmica vermelha. *Cerâmica Industrial*, **22**, 41-49. https://doi.org/10.4322/cerind.2017.029

[24] Faria, O.B. (2002) Utilização de macrófitas aquáticas na produção de adobe: Um estudo de caso no reservatório de Salto Grande (Americana-SP). Ph.D. Thesis, Universidade de São Paulo.

[25] Celik, H. (2010) Technological Characterization and Industrial Application of Two Turkish Clays for the Ceramic Industry. *Applied Clay Science*, **50**, 245-254. https://doi.org/10.1016/j.clay.2010.08.005

[26] Daghmehchi, M., Rathossi, C., Omrani, H., Emami, M. and Rahbar, M. (2018) Mineralogical and Thermal Analyses of the Hellenistic Ceramics from Laodicea Temple, Iran. *Applied Clay Science*, **162**, 146-154. https://doi.org/10.1016/j.clay.2018.06.007

[27] Taguchi, S.P., Santos, J.C., Gomes, T.M. and Cunha, N.A. (2014) Avaliação das propriedades tecnológicas de cerâmica vermelha incorporada com resíduo de rocha ornamental proveniente do tear de fio diamantado. *Cerâmica*, **60**, 291-296. https://doi.org/10.1590/s0366-69132014000200020

[28] Vitorino, J.P.D., Monteiro, S.N. and Vieira, C.M.F. (2009) Caracterização e incorporação de resíduos provenientes de estação de tratamento de água em cerâmica argilosa. *Cerâmica*, **55**, 385-392. https://doi.org/10.1590/s0366-69132009000400008

[29] Callister, W.D. and Rethwisch, D.G. (2013) Materials Science and Engineering: An Introduction. John Wiley and Sons.

[30] NM 127 (2009) Tijolos—Especificações e métodos de ensaio. Ed. 1, 24 p.